12.5 Implementation and Evaluation of a New Shallow Convection Scheme in WRF

Aijun Deng* and Brian Gaudet
Department of Meteorology, The Pennsylvania State University

Jimy Dudhia
National Center for Atmospheric Research

Kiran Alapaty
United States Environmental Protection Agency

1. INTRODUCTION

Clouds are well-known to be a crucial component of the weather and climate system since they transport heat, moisture and momentum vertically in the atmosphere, and strongly modify shortwave and longwave radiation budgets. From the air quality point of view, cloud processes, in particular those associated with shallow cumulus clouds, can play a major role in ventilating air pollutants from the planetary boundary layer (PBL) to the free atmosphere, causing them to be transported away along the mean flow. However, accurate representation of cloud processes remains one of the challenges in atmospheric models, especially in global numerical weather prediction (NWP) and climate models. Despite great computational advances, calculations using global NWP and climate models are generally performed using relatively coarse grid spacing such that cloud processes remain unresolved. Thus the effect of moist convection must be represented by parameterizations. Increased model resolution resolves some significant parameterization issues. However, cloud parameterization development will remain a key need in the foreseeable future for a variety of reasons, one of which is that the computational expense of cloud-resolving models makes their routine use in seasonal and climate prediction as well as in ensemble prediction systems still several decades away (Jakob 2010).

In past decades, most subgrid-scale cloud research in numerical modeling has focused on deep convection. Shallow convection parameterization (SCP) received less attention until mid-1990s when pioneering research on shallow convection parameterization for mesoscale models (Deng 1999, Deng et al. 2003a and Deng et al. 2003b) was conducted at Penn State University (PSU) using the Penn State/National Center for Atmospheric Research (NCAR) Mesoscale Model -- MM5 (Grell et al 1994), followed by SCP research conducted at the University of Washington (UW, Bretherton et al. 2004). Both the Deng et al. (hereafter referred as PSU SCP or PSU-Deng SCP) and Bretherton et al. (hereafter referred as UW SCP) SCP schemes are mass-flux based convective parameterization schemes, and both use a triggering function based on boundary-layer properties and a buoyancy-sorting approach similar to the Kain-Fritsch (1990, 1993) deep convection scheme. The PSU SCP scheme uses a hybrid closure that smoothly transitions from an approach based solely on the boundary layer turbulent kinetic energy (TKE) to one based on CAPE removal as the depth of the convective layer deepens. Also of importance, the PSU SCP scheme has physically-based prognostic equations to predict cloud fraction and subgrid cloud water that can interact with atmospheric radiation to produce more realistic cloud radiation forcing, unlike many other schemes in which cloud fraction is diagnosed.

The PSU-Deng SCP scheme, along with Penn State Gayno-Seaman (PSU-GS) PBL scheme, is being implemented into the Weather and Research Forecasting (WRF) model, and has been tested in the WRF single column model (SCM) over the same three convective cases documented in Deng et al. 2003b: 1) a marine stratus case from the Atlantic Stratocumulus Transition Experiment; 2) a continental shallow cumulus and stratocumulus; and 3) a continental deep convection. It was found that for all three different convective environments, WRF with the PSU-Deng SCP scheme is able to reproduce the major features of the MM5 results, including the cloud depth, fraction and cloud water (Deng et al. 2013).

Following the SCM testing and evaluation, a 3-D WRF simulation was conducted over a postfrontal shallow cumulus case over the northeastern U.S. This paper describes the test results from this continental shallow convective case. In order to demonstrate that the PSU SCP scheme is flexible and works with different TKE-based PBL schemes, a sensitivity study using the 2.5 level TKE-based MYNN PBL scheme is performed. For the same shallow cumulus case, the PSU SCP scheme is compared with the UW SCP scheme, a well-established SCP scheme that has been implemented into the Community Earth System Model (CESM) and widely used by the climate community, and that is now also in WRF making such a comparison study possible. Section 2 of the paper gives an overview of the PSU-Deng SCP scheme, and Section 3 briefly describes the WRF model used in this study. The test case description is given in Section 4 and the model configuration is discussed in Section 5. Model results and discussions are given in Section 6 and 7, and a summary and conclusions are given in Section 8.

2. OVERVIEW OF PSU SHALLOW CONVECTION SCHEME

As is typical of mass flux-based parameterization schemes, the PSU SCP scheme is comprised of three

*Corresponding Author: Aijun Deng, Department of Meteorology, 503 Walker Building, Pennsylvania State University, University Park, PA 16802; email: axd157@psu.edu

major components: 1) cloud triggering, 2) plume model driven by parcel buoyancy, and 3) closure assumption. In the PSU SCP scheme convection is triggered by the combination of the grid-resolved upward motion and the TKE within the model-predicted boundary layer representing the subgrid-scale turbulence, and a non-hydrostatic "pumping" contribution when the cloud depth is greater than 4 km. The size of an individual updraft (currently assumed to be uniform in radius) is proportional to the updraft depth and to the PBL depth. That is a deeper cloud has a larger-sized radius and the cloud grows larger in radius as the PBL depth grows (a mathematic relationship among cloud radius, updraft radius and PBL depths is given in Deng et al. 2003a). The closure assumption of the PSU SCP is based on a hybrid approach that combines the use of PBL TKE and CAPE depending on the depth of the convective updraft. When the updraft top is lower than the level of free convection (LFC), (i.e., shallow clouds), the amount of convection is determined by the amount of TKE in the lower PBL. When the depth of updraft is higher than 4 km (deep clouds) the number of updrafts is determined by the CAPE in the entire atmospheric column, similar to the mechanism used in the Kain-Fritsch (KF, Kain and Fritsch 1990, 1993, and Kain 2004) cumulus parameterization scheme (CPS). When the updraft top is higher than the LFC but the updraft depth is smaller than 4 km, the number of updrafts is determined by a weighted average between the shallow and deep convection values-a hybrid of TKE and CAPE approach.

In addition to the updraft formulation, the PSU SCP also contains two predictive equations for cloud fraction (a*)* and cloud liquid/ice water content (l_c) for neutrally-buoyant clouds (NBC), dead clouds detrained from the active updraft core (Deng et al. 2003a). As shown in Fig. 1, the NBC sources terms are determined by the rate of updraft detrainment. Dissipation processes include evaporation due to mixing at the sides of the cloud, the depletion of water liquid/ice content due to vertical mixing, cloud water depletion due to precipitation (drizzle), a depletion rate contributed by an ice settling process, and cloud water depletion due to cloud-top entrainment instability. NBCs can be advected away from the updraft locations by the resolved flow. However, NBC advection processes (both horizontal and vertical) are not yet implemented.

As shown in Fig. 2, WRF-predicted NBC fraction can be either greater or smaller than the cloud updraft fraction that only occupies a very small portion of the grid volume (i.e., < 5% in this case), depending on balance between cloud updraft detrainment and entrainment as well as the environment conditions. WRF-predicted NBC water content is smaller than the updraft value. Since in the real atmosphere, clouds by no means are precisely overlapping in the vertical, it is reasonable to assume the actual cloud fraction is greater than that predicted NBC fraction. Therefore, to radiation calculation, PSU-Deng SCP introduced a correcting factor to expand the NBC fraction. Such a factor is proposed in Deng et al. (2003a) to combine the SCP-predicted cloud fraction and the cloud fraction based on the Xu and Randall (1996) formulation determined by relative humidity. This factor may not be needed if NBC advection processes are implemented, although further investigation is needed.

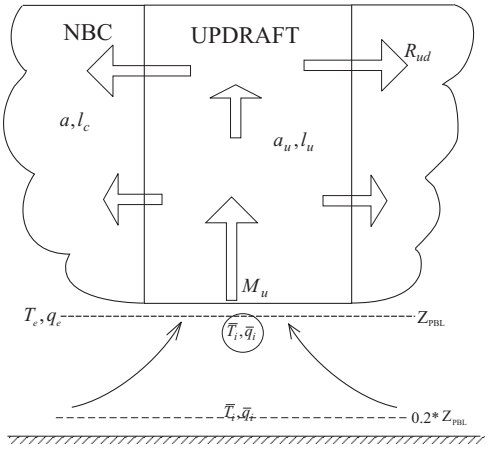

Figure 1*. Schematic of the PSU-Deng SCP, where a is the neutrally-buoyant cloud (NBC) fraction, l_c is the NBC cloud water content, l_u is the cloud water content in the updraft and a_u is the updraft fraction, denoted by subscript u, R_{ud} is the updraft detrainment rate, and Z_{PBL} is the depth of the PBL.*

It is important for the atmospheric radiation calculation to make use the NBC fraction and water content predicted by the PSU-Deng SCP scheme. Some of the newer radiation schemes (e.g., RRTMG in WRF, Iacono et al. 2008) consider partial cloudiness when radiation tendencies are calculated in the atmospheric column, which eliminates the need for running the radiation scheme multiple times as proposed in Deng et al. (2003a). It is worth noting that the PSU SCP scheme can smoothly transition to the KF deep convection scheme when the updraft is deep enough. The subgrid NBCs produced by the SCP scheme can smoothly transition to explicit clouds when the grid cell becomes saturated.

3. MODEL DESCRIPTION

The WRF modeling system is a state-of-the-science community-supported numerical weather prediction (NWP) and atmospheric simulation system used worldwide for both research and operational applications (Skamarock et al. 2008). WRF's development is supported by the broad scientific community, along with very active participation of university scientists worldwide. WRF has a flexible, portable code that runs efficiently in computing environments ranging from massively parallel supercomputers and clusters to laptops. It is designed for simulating atmospheric phenomena across scales ranging from large eddies (~100 m) to mesoscale circulations and waves (~ 1 km to 100 km) to synoptic-scale weather systems (~1000 km). These applications include real-time NWP, model physics research, regional climate simulation, air-quality and hazard prediction modeling, etc.

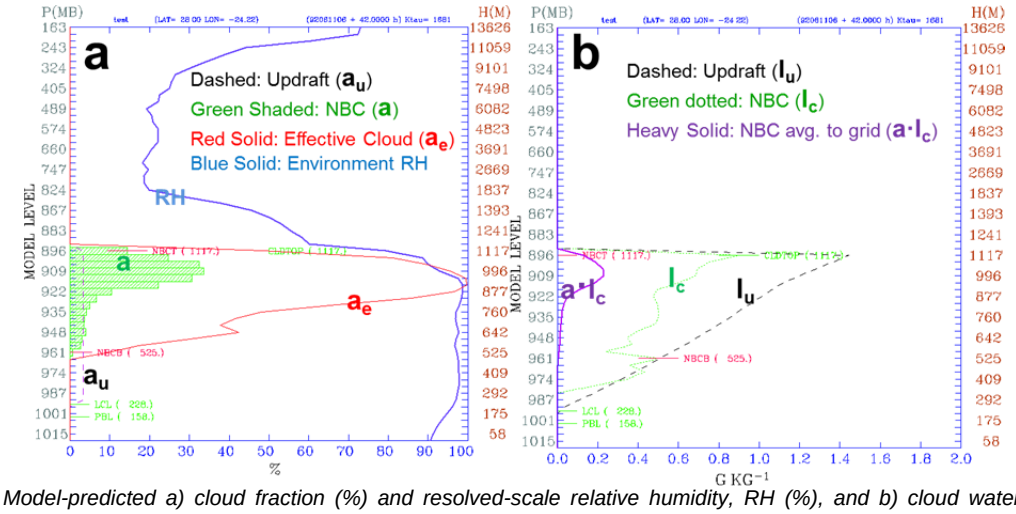

***Figure 2**. Model-predicted a) cloud fraction (%) and resolved-scale relative humidity, RH (%), and b) cloud water content vs. pressure (hPa) and height (m) at 1200 UTC 11 Jun 1992 (model forecast hour 5) for ASTEX at 28.008N, 24.228W. On the left panel shading indicates NBC fraction (a, %), the dashed line is the fraction of cloud updraft (a_u, %), the thin solid curve is the effective cloud area for radiation calculations (a_e, %), and the heavy curve is RH (%). On the right panel, thin dashed curve shows the NBC water content (l_c), dashed shows the cloud updraft water content(l_u), and thick solid curve shows the NBC water content averaged onto the resolved scale. LCL denotes the lifting condensation level, PBL is the boundary layer top, CLDTOP is the top of updraft, and NBCT and NBCB are the top and base of NBCs, respectively. The numbers in parentheses indicate the height (m AGL) of the labeled item.*

The WRF model includes a complete suite of atmospheric physical processes that interact with the model's dynamics and thermodynamics core. These physical processes include cloud microphysics (MP), cumulus parameterization, atmospheric radiation, planetary boundary layer (PBL)/turbulence physics, and land surface processes. The WRF modeling system also has four-dimensional data assimilation (FDDA) capabilities to allow the meteorological observations to be assimilated into the model (Deng et al. 2009), although FDDA is not applied in this study.

4. TEST CASE DISCRIPTION

To evaluate the PSU-Deng SCP using WRF with full 3-D configuration, a postfrontal continental shallow cumulus case over the eastern U.S is selected. As shown in in Fig. 3 the entire region was clear in the early morning at 12 UTC, 30 July 2013, except for the cloud system associated with the front moving eastward offshore. As the day progressed, shallow cumulus clouds started to develop across the region, with quite extensive coverage observed in the early afternoon at 18 UTC, 30 July 2013, and then starting to dissipate in the late afternoon through night time. The ground global horizontal irradiance (GHI) observed at the Penn State Rock Springs Research Farm facility shows clear signals of shallow cumulus clouds propagating across site, with the majority of cloud activity occurring between 15 through 21 UTC, and with very little clouds between 21 UTC, 30 July and 00 UTC, 31 July. The national 24-hour precipitation maps for both 12 UTC, 30 July and 12 UTC, 31 July show that a cold font had passed and pushed into the Atlantic Ocean. The entire study region over the Eastern U.S is precipitation free.

5. MODEL CONFIGURATION AND EXPERIMENT DESIGN

The WRF model used in this research (both implementation and model testing and evaluation) is based on the WRF V3.5.1 released in September 2013. Since the original SCP scheme was developed and only tested in MM5 with a coarse resolution – a resolution that is commonly used by global NWP models, our first attempt was to test it with a similar grid configuration. Figure 4 shows a single grid with grid spacing of 36 km, and 100x100 grid points in horizontal. In the vertical, fifty (50) vertical terrain-following layers are used, with the center point of the lowest model layer located ~10 m above ground level (AGL). The thickness of the layers increases gradually with height, with 27 layers below 850 hPa (~1550 m AGL). The top of the model is set at 100 hPa. The initial and lateral boundary conditions used in this study were based on the National Centers for Environmental Prediction global forecast system (GFS). The GFS 0.5-degree gridded forecast fields initialized at 12 UTC, 30 July 2013 were used. No FDDA is used in all WRF simulations.

Table 1: Experimental Design

	Exp Name	PBL	SCP	CPS	MP
Baseline Evaluation	NoShCu	PSU-GS	N/A	KF	WSM3
	ShCu	PSU-GS	PSU-Deng	N/A	WSM3
Sensitivity Evaluation	NoShCu	MYNN	N/A	KF	WSM3
	ShCu	MYNN	PSU-Deng	N/A	WSM3
Comparison Evaluation	NoShCu	UW PBL	N/A	KF	CAM5
	ShCu	UW PBL	UW	KF	CAM5

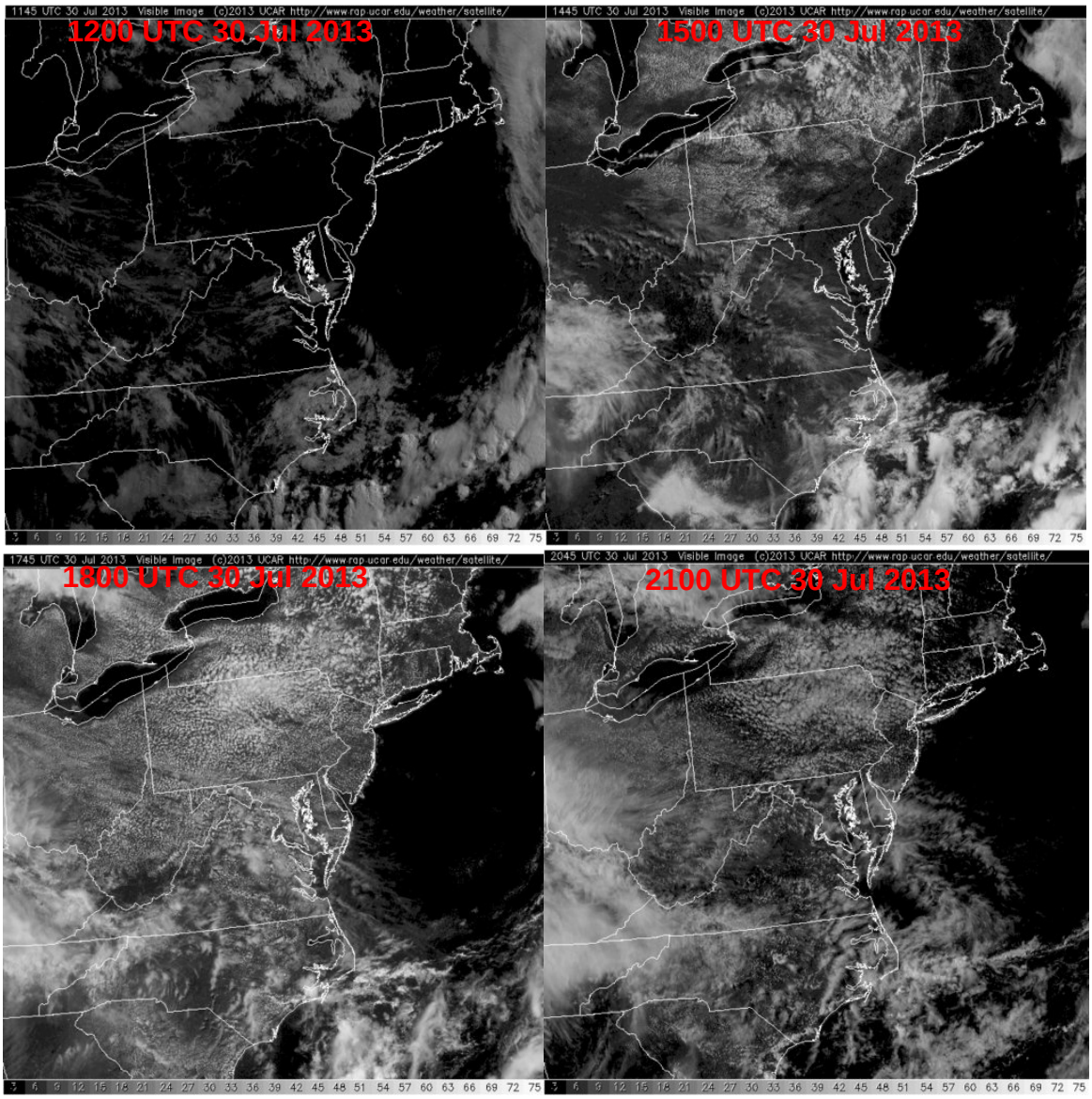

***Figure 3**. GOES visible satellite imagery at 3 h intervals for 30 July 2013 over the East Coast. Courtesy UCAR/RAL.*

As shown in Table 1, three sets of evaluation are performed. The model physics options used in a baseline evaluation of the PSU SCP are similar to those used in MM5. These physics options include use of PSU-GS PBL scheme (Shafran et al. 2000), WSM 3-class simple ice microphysics scheme, and a simple force-restore model, or thermal diffusion LSM, for land surface processes. For atmospheric radiation, the RRTMG scheme is used in all the simulations since it is designed to allow interaction between partial cloudiness and atmospheric radiation. For the cumulus parameterization scheme, either the KF CPS or the PSU-Deng SCP is used.

Following the baseline evaluation, a sensitivity evaluation is configured to verify that the PSU SCP is flexible and works with a different TKE-based PBL scheme. Therefore the sensitivity evaluation is configured identically to the baseline evaluation except that instead of using the PSU-GS PBL scheme, the 2.5-level TKE-based MYNN PBL is used. Other physics options used include RRTMG radiation, WSM3 MP, thermal diffusion LSM, and KF CPS or PSU-Deng SCP.

In this study, the PSU SCP scheme is compared with the UW SCP scheme, a well-established SCP scheme. Therefore a comparison evaluation is configured to use the UW SCP scheme. Since the UW SCP scheme requires the use of the UW PBL scheme and Community Atmospheric Model 5 (CAM5) MP (both are available in WRF), in the comparison evaluation, all three are used. Note that unlike the PSU SCP scheme that parameterizes both shallow and deep convection, the UW scheme only parameterizes shallow convection, and separate deep convection parameterization is needed. In order to fairly compare to the baseline evaluation and sensitivity evaluation, KF CPS is used for

deep convection in simulations in which UW physics is used or in simulations in which PSU SCP is not used.

For each of the three evaluations, two WRF simulations are compared: 1) NoShCu in which no shallow convection parameterization is used but a deep convection parameterization (i.e., KF SCP) is used and 2) ShCu in which both shallow and deep convection is used. Comparison between the No ShCu and the ShCu simulations will show the added value of the SCP scheme. All simulations are 24 hours long, starting at 12 UTC, 30 July and ending at 12 UTC, 31 July 2013.

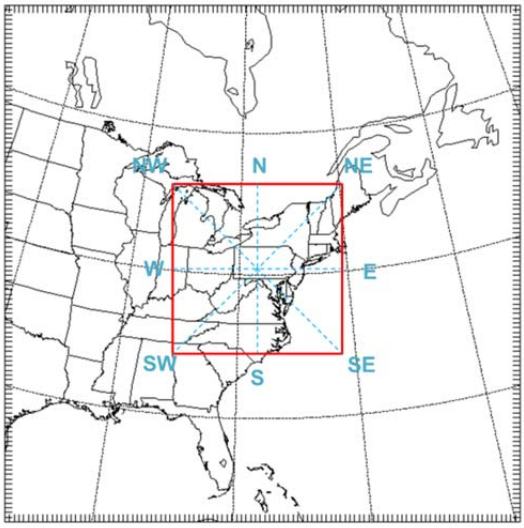

Figure 4*. WRF grid configuration with 36-km horizontal spacing. The inner box approximately represents the area covered by the satellite image, and dashed lines indicate the locations from which model cross-sections are created.*

6. MODEL RESULTS

Model results are evaluated both qualitatively and quantitatively. Quantitative evaluation is performed by comparing the error statistical scores of the model-simulated wind speed, wind direction, temperature (T), and RH. Since shallow convection mainly redistributes heat and moisture in vertical, we will only focus on the quantitative evaluation of mass fields. Mean absolute error (MAE) is calculated to measure how close the model values are compared to the observed values. Mean error (ME) is calculated to measure the model bias for a given variable. MAE and ME are computed for both surface and upper air. For surface, the model values from the lowest model layer are compared with the surface observations. For upper air, the model values are interpolated onto the observation locations in both horizontal and vertical pressure space, and are then compared with the observations. Qualitative evaluation is performed by examining the WRF-predicted cloud fields, as well as the associated surface temperature and radiation fluxes. Cross sections (locations are shown in Fig.4) of the WRF-predicted NBC fraction and water content and their variation with time are qualitatively examined. Surface global horizontal irradiance (GHI) is compared between the predicted and the observed values.

6.1 Baseline Evaluation

Figs. 5a and 5b show the vertically integrated resolved-scale cloud water at 21 UTC, 30 July 2013, comparing the No ShCu and Shcu simulations in the baseline evaluation. As expected, there is little difference in terms of resolved clouds, and the cloud coverages are slightly larger in NoShCu simulation due to the fact that there are subgrid clouds predicted by WRF when the PSU SCP is used. Figs. 5c and 5d show subgrid NBC cloud fraction and cloud water at ~2-km AGL at the same time. Consistent with the observation shown in Fig.3, the northeast United States has dominant shallow cumulus with cloud fraction less than 100%, with some areas of ~70% cloud coverage over PA. The cloud free areas over the lakes in Fig. 5c and 5d are well represented in WRF due to lack of TKE (not shown) that is responsible for triggering cloud updrafts.

In order to examine the 3-D structure of the WRF-predicted NBC cloud fields, several cross sections were created (i.e., W-E, S-N, NW-SE and SW-NE in Fig. 4), with only a few cross sections shown in this paper. Figure 6 shows the southwest-northeast cross section of the WRF-predicted NBC cloud fields and TKE in the ShCu simulation in the baseline evaluation. It is shown that in late morning at 3 h (15 UTC or 11 AM, Fig. 6a) the atmospheric boundary layer is still shallow (only a few hundred meters) with little TKE, especially to the southwestern side of the cross section. Note that the horizontal variation of the TKE distribution or PBL depth is likely the result of difference in the surface solar radiation fluxes (or sun angles). The NBC cloud fraction at this time is quite small, less than 20% with the maximum cloud water content of ~1 kg kg^{-1}. Cloud base is generally near the top of the PBL where TKE drops off. As the PBL continues to grow and TKE increases at later times, cloud fraction and cloud water contents both increase, as well as the heights of cloud base. At 6 h (18 UTC or 2 PM, Figure 6b), cloud fraction increased to above ~30%, along with larger cloud water content. At 9h (21 UTC or 5 PM, Fig. 6c), PBL starts to weaken, with smaller amount TKE compared with 6 h time, and cloud fraction reached above 40%, but with decreased cloud water content. At 12 h (00 UTC or 8 PM, Fig. 6d), PBL has collapsed. Due to lack of source terms from updrafts that are triggered by the low-level TKE in the PBL, NBC clouds start to dissipate. Both NBC cloud fraction and water content are decreased compared to the earlier time.

At night times as the PBL disappears, clouds continue to dissipate. Figure 7 shows the same southwest-northeast cross section of the WRF-predicted NBC cloud fields and TKE for four night times in the ShCu simulation in the baseline evaluation. It is shown that both cloud fraction and cloud water content decreases as time progresses, although some near-surface clouds (or fog) persisted associated with the TKE, likely generated by wind shear near the surface. Notice that there is TKE aloft in the cloud layer which can cause cloud to dissipate through cloud top entrainment instability. Since we don't have satellite

images for night times to verify the cloud amount, it is unclear that these leftover clouds are consistent to the observations. However, it is worth pointing out that PSU-Deng SCP scheme currently does not have NBC advection processes implemented, and it is not hard to imagine that clouds can evaporate faster if they are advected to drier environment.

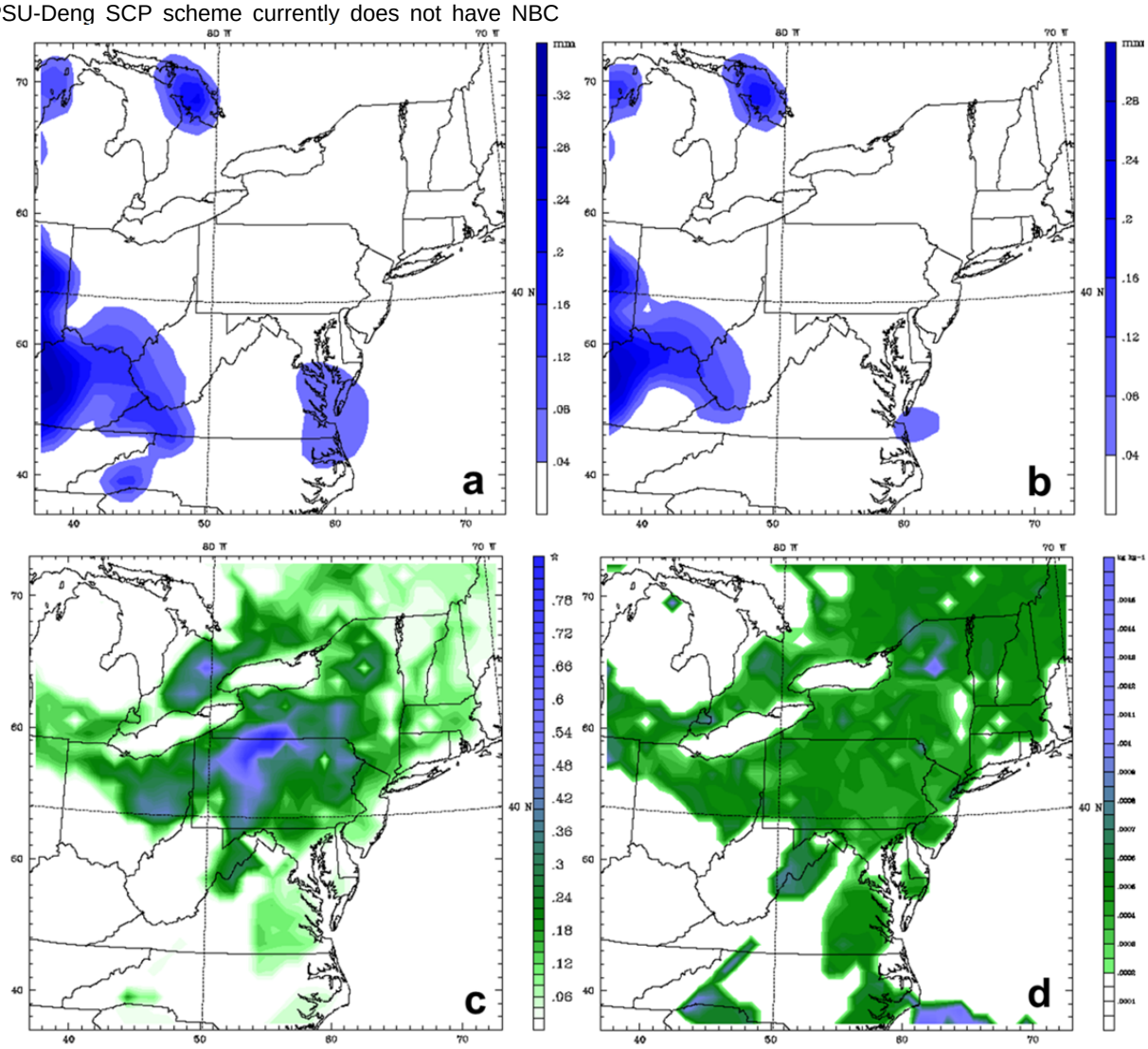

Figure 5. *WRF-predicted cloud fields at 21 UTC, 30 July 2013: a) and b) vertically integrated resolved-scale cloud water (mm) for both NoShCu and ShCu simulations, respectively; c) partial cloud fraction at ~2-km AGL in ShCu simulation; and d) partial cloud water content (kg/kg) at ~2-km AGL in ShCu simulation.*

As mentioned earlier, the RRTMG radiation scheme allows interaction between the fractional (or partial) clouds and radiation calculations to produce improved atmospheric radiation fluxes. The added value of the PSU-Deng SCP can be evaluated by comparing the WRF-predicted surface solar irradiance between the NoShCu and ShCu simulations. Figure 8 shows a comparison of the WRF-predicted GHI the two simulations at 21 UTC, 30 July 2013. It is evident that there is less solar energy reaching the ground in the ShCu simulation due to the presence of partial clouds in ShCu. For example the solar irradiance values over northeastern PA and southern NY in NoShCu are between 600 and 800 W m^{-2}, while they are less than 200 W m^{-2} in some regions in ShCu. To demonstrate that WRF with the PSU SCP reasonably predicts the surface GHI, Fig. 9 shows the observed GHI (Fig. 9a) and WRF-predicted GHI (Fig. 9b) at the Penn State Rock Springs facility between 12 UTC 30 July 2013 and 00 UTC 31 July 2013. The observed GHI clearly shows cloud activity over the Rock Springs site, with the cloud starting time agreeing with the ShCu simulation. Notice that based on the observed 1-min values, the observed GHI values are in the range between 200 and 900 W m^{-2} that are well represented in the GHI values across the simulation domain (Fig. 8b). Since the model solution represents the values average over the entire 36-km grid box in this case, a fair comparison would require a time average over the observed 1-min GHI. The green curve in Fig. 9a represents the 90-min averaged values of the observed GHI (based on the use of Taylor's hypothesis

for a 36-km grid cell and approximately 7 m s^{-1} wind speed), indicating that WRF with PSU SCP does an overall good job in predicting the ground GHI.

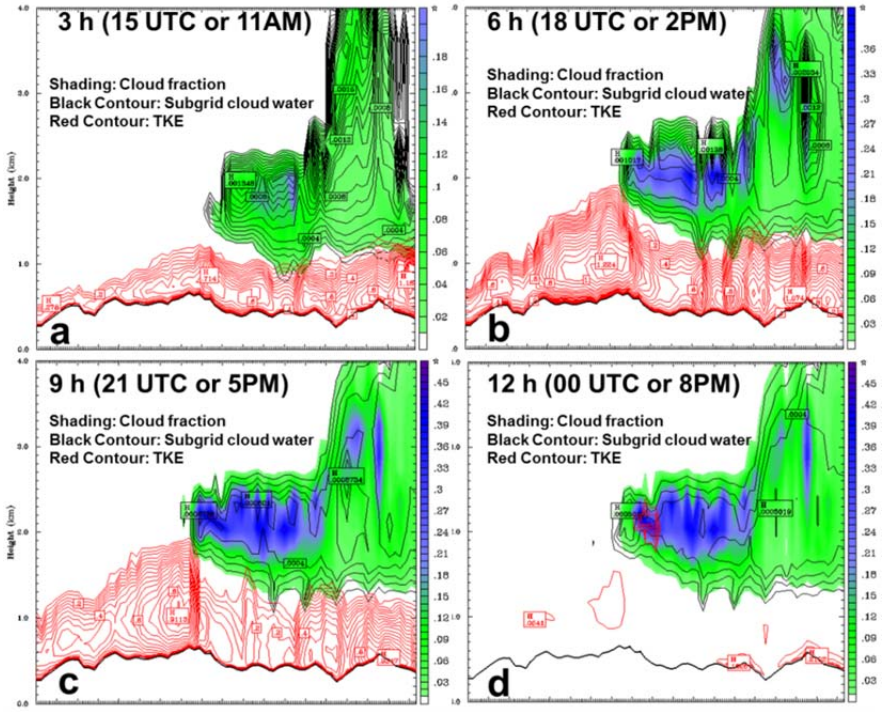

Figure 6. *Southwest-Northeast cross section showing WRF-predicted NBC cloud fields and TKE in ShCu simulation in the baseline evaluation, for a) 3 h, b) 6 h, c) 9 h and d) 12 h time. Color shading: cloud fraction; black contour: cloud water content (kg kg^{-1},with interval 0.0001); red contour: TKE (m^2 s^{-2}, with interval 0.05).*

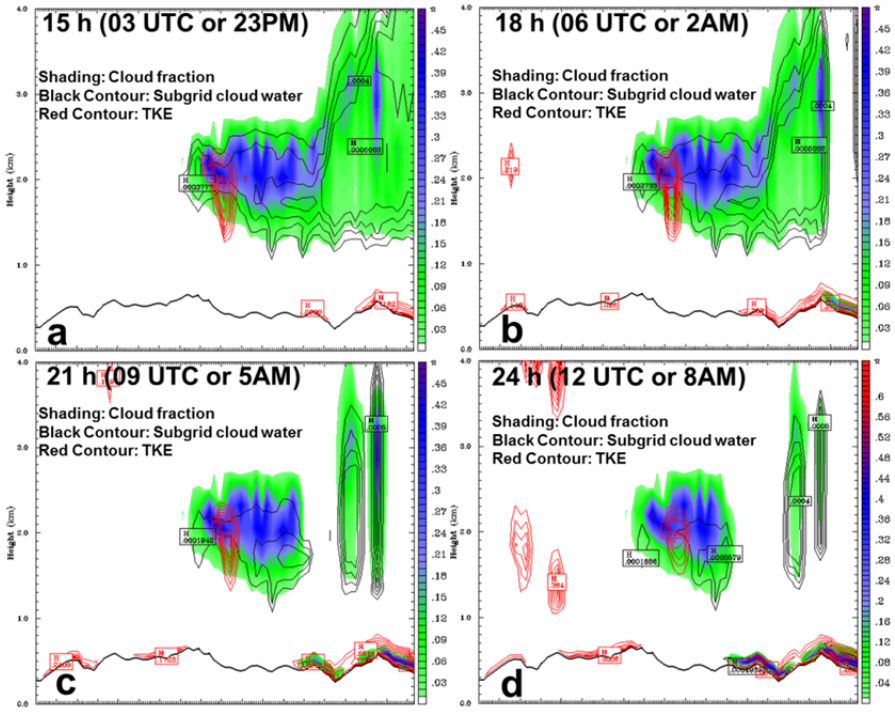

Figure 7. *Southwest-Northeast cross section showing WRF-predicted NBC cloud fields and TKE in ShCu simulation in the baseline evaluation, for a) 15 h, b) 18 h, c) 21 h and d) 24 h time. Color shading: cloud fraction; black contour: cloud water content (kg kg^{-1},with interval 0.0001); red contour: TKE (m^2 s^{-2}, with interval 0.05).*

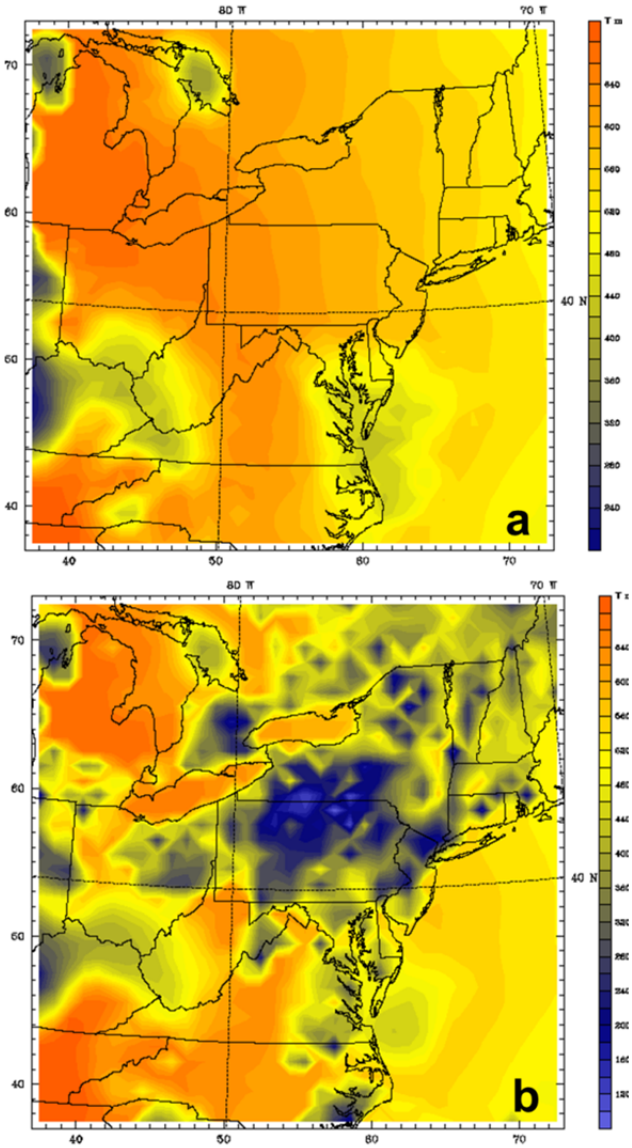

Figure 8 *WRF-predicted surface global horizontal irradiance (GHI, W m^{-2}) at 9h (21 UTC, 30 July 2013), for a) NoShCu simulation and b) ShCu simulation in the baseline evaluation.*

Atmospheric convection plays a major role in vertically redistributing heat and moisture through convective process such as updraft, downdraft and subsidence. The effect of a parameterization scheme can be evaluated by validating the model solutions against the observed meteorological conditions. During the simulation period, within the entire model domain, there are about 2000 WMO surface observations available at a given hour, and there are about 60 upper-air observations at 00 or 12 UTC times. Both mean absolute error (MAE) and mean error (ME) are computed over the entire simulation grid.

Figure 10 shows the model error of the WRF-predicted surface-layer temperature and relative humidity as a function of time. It is shown that for temperature, ShCu clearly shows smaller MAE throughout the entire 24-h simulation. The temperature ME scores show that WRF without the SCP scheme has a warm bias which is reduced by the use of the SCP scheme. This conclusion based on surface temperature verification seems to be supported by the fact that there is less solar radiation reaching the ground in the ShCu simulation as shown in Fig. 8 due to the presence of partial cloudiness. Similarly, for the WRF-predicted RH field, there is an MAE reduction in ShCu simulation, but mostly in the night time, which is consistent with the ME distribution which also shows there is a reduced moisture bias during this time period

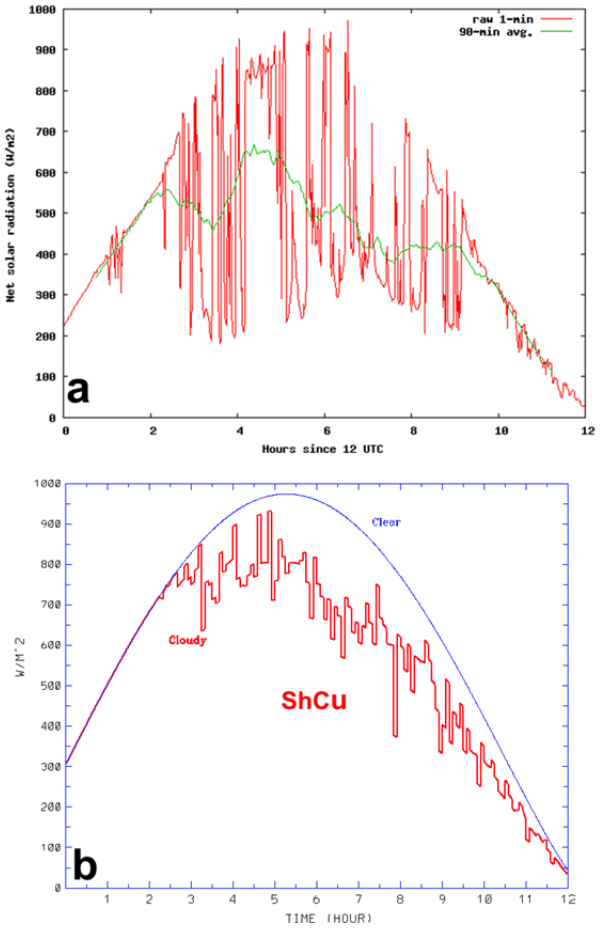

Figure 9. *a) Observed GHI and b) WRF-predicted GHI (W m^{-2}) at Penn State Rock Springs facility between 12 UTC 30 July 2013 and 00 UTC 31 July 2013. The red solid curve on the left panel with higher frequency oscillations shows the values with 1-min sampling and green solid curve shows the 90-min averaged from the 1-min samples. The red curve on the right shows the mode-predicted GHI by WRF using the PSU SCP scheme and the blue curve on the right panel shows the WRF-predicted clear-sky values.*

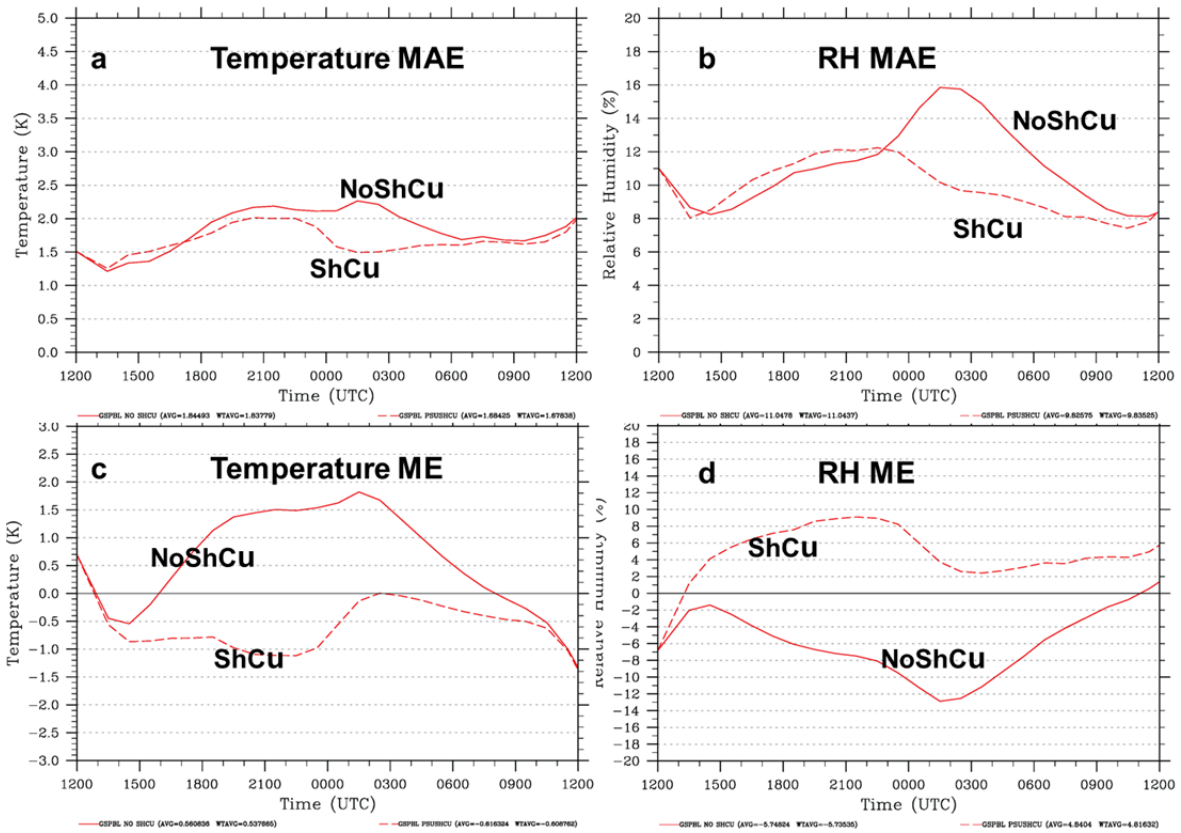

Figure 10. *Model error of the WRF-predicted surface-layer temperature and relative humidity as a function of time, for a) Temperature MAE, b) RH MAE, c) Temperature ME, and d) RH ME.*

Figure 11 shows the model error of the WRF-predicted temperature and relative humidity as a function of height near the end of the daytime period, at 12 h (00 UTC, 30 July 2013). For temperature, MAE scores in ShCu show systematic error reduction throughout the entire atmosphere, with somewhat larger reductions (~0.5 K) in the lower atmosphere. More evident error reduction is seen in the temperature ME scores in the lower atmosphere where ~2-K bias at the surface in the NoShCu is almost completely removed in the ShCu simulation. For RH, the MAE scores in both simulations are quite close, except that near the surface ShCu has a smaller MAE by a few percent. Similar to the temperature ME, there appears to be a larger separation between the two simulations near the surface, and the ShCu simulation has smaller bias.

6.2 Sensitivity Evaluation

As described earlier, the sensitivity evaluation is configured identically to the baseline evaluation except that instead of using the PSU-GS PBL scheme, the 2.5-level TKE-based MYNN PBL is used. The model solutions for both NoShcu and ShCu simulations in the sensitivity evaluation are found to be quite similar to those in the baseline evaluation. For example, Fig. 12 compares the WRF-predicted NBC cloud fields and TKE in ShCu simulation between the baseline evaluation (top) and the sensitivity evaluation (bottom) for both 3 and 6 h times. Although the TKE patterns are similar, the PBL depths predicted by the PSU GS PBL scheme appear to be lower than those predicted by the MYNN PBL scheme, indicating more vigorous vertical mixing in the MYNN PBL scheme. Despite the difference in the PBL structure, the WRF-predicted NBC cloud fields overall appear to be similar. For both times, the cloud base heights are comparable between the baseline and sensitivity evaluation. The cloud fraction appears to be greater in the baseline, but its horizontal and vertical extent is greater in the sensitivity simulation with the MYNN PBL scheme, indicating that the overall cloud amount and their effects may be similar. This hypothesis seems to be confirmed by the WRF-predicted GHI (W m^{-2}) at Penn State Rock Springs facility between 12 UTC 30 July 2013 and 00 UTC 31 July 2013 (Fig. 13). Comparing Fig 13 and Fig. 9b, we notice that cloud amount in both baseline and sensitivity simulations are quite comparable, with slightly larger amount of clouds in the sensitivity simulation when the MYNN PBL scheme is used.

6.3 Comparison Evaluation

In the comparison evaluation, WRF is configured to use the UW SCP scheme, along with the UW PBL scheme and CAM5 MP. In the UW SCP scheme the cloud fraction is diagnosed through its combination with a specific microphysics scheme (i.e., CAM5

microphysics). Unlike the PSU SCP that can parameterize both shallow and deep convection, the UW SCP scheme requires additional deep convection parameterization. In order to fairly compare to the baseline evaluation, KF CPS is used for deep convection here. Figure 14 shows the WRF-predicted GHI at the Penn State Rock Springs facility between 12 UTC 30 July 2013 and 00 UTC 31 July 2013. It is shown that WRF with UW SCP produced very little clouds although clouds start at the same time as in the baseline and sensitivity simulations. Since cloud fraction predicted by the UW SCP scheme interacts with the atmospheric radiation calculation through the CAM5 microphysics scheme, it would be interesting to evaluate a simulation with the UW SCP scheme tuned off. As shown in Fig. 14, the CAM5 microphysics scheme seems to produce more clouds which are reduced when the UW SCP scheme is used.

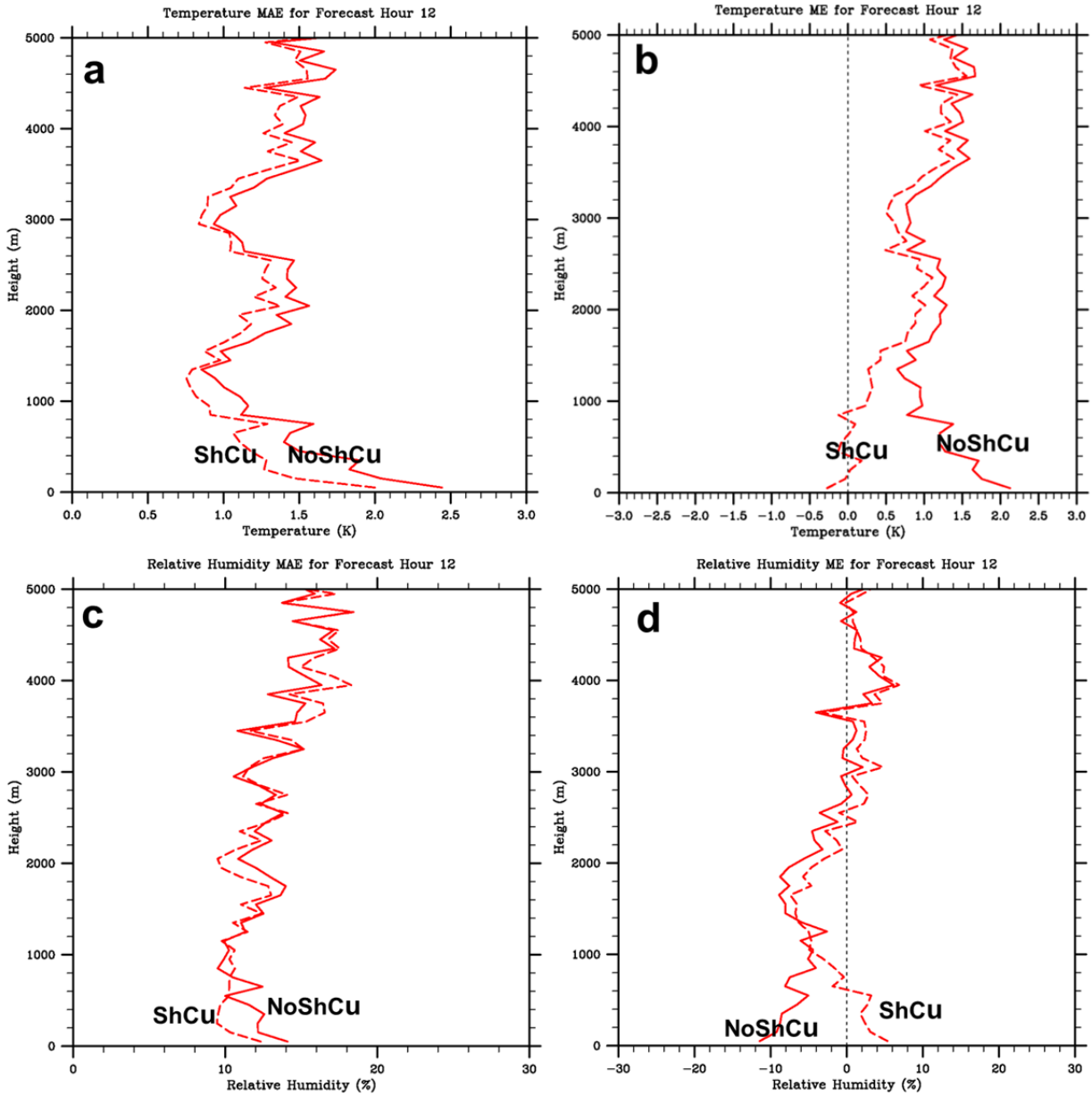

Figure 11. *Model error of the WRF-predicted temperature and relative humidity as a function of height at 12 h (00 UTC, 30 July 2013), for a) Temperature MAE, b) Temperature ME, c) RH MAE, and d) RH ME, comparing between NoShCu (solid) and ShCu (dashed).*

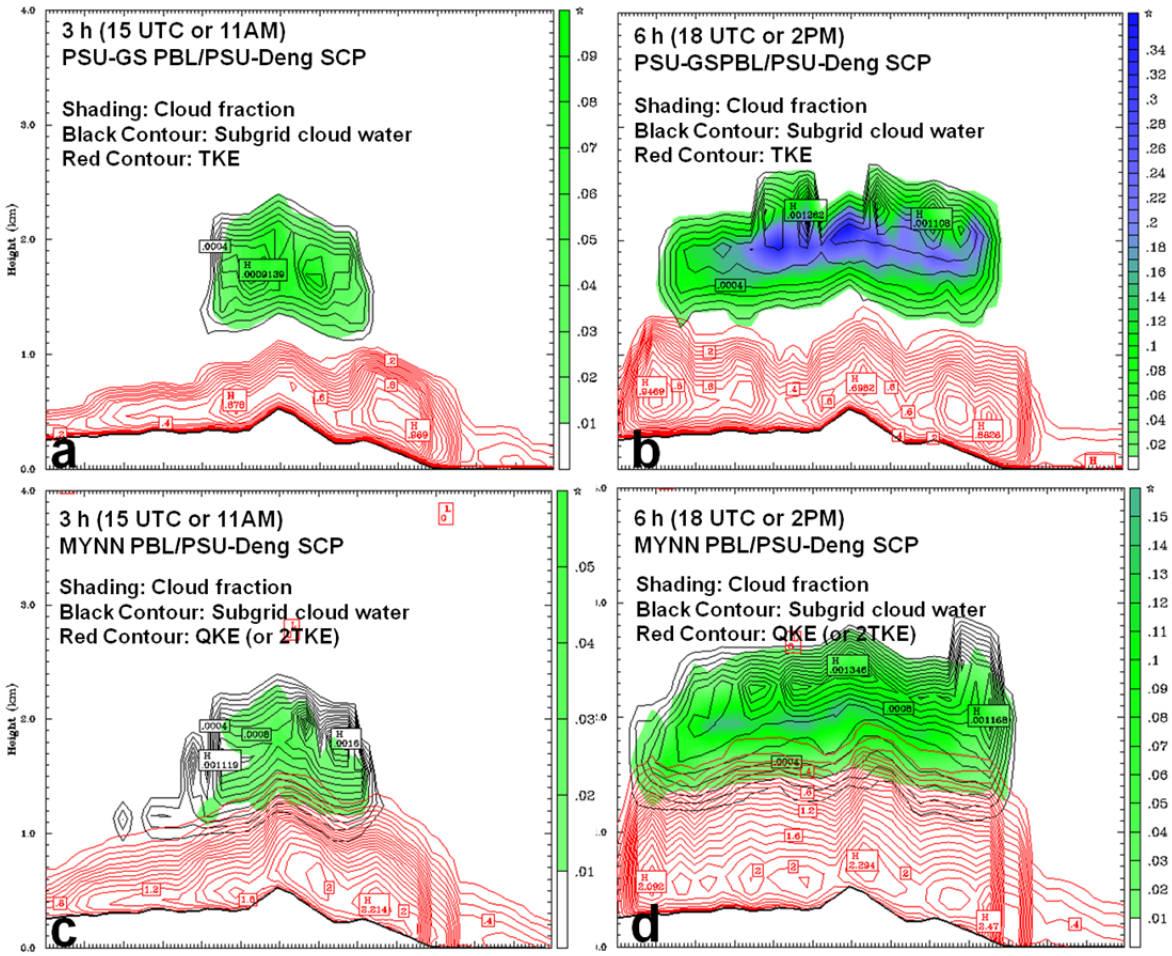

Figure 12. *West-East cross section showing WRF-predicted NBC cloud fields and TKE in ShCu simulation comparing the baseline evaluation (top) and the sensitivity evaluation (bottom), for 3 h (a and c), and 6h (b and d) times. Color shading: cloud fraction; black contour: cloud water content (kg kg^{-1},with interval 0.0001); red contour in top panels: TKE (m^2 s^{-2}, with interval 0.05); red contour in bottom panels: QKE or twice TKE (m^2 s^{-2}, with interval 0.1);*

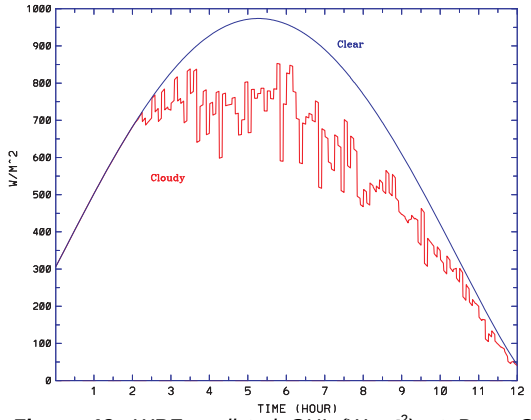

Figure 13. *WRF-predicted GHI (W m^{-2}) at Penn State Rock Springs facility between 12 UTC 30 July 2013 and 00 UTC 31 July 2013. The red curve shows the mode-predicted GHI by WRF using the PSU SCP scheme but with MYNN PBL scheme and the blue curve shows the WRF-predicted clear-sky values.*

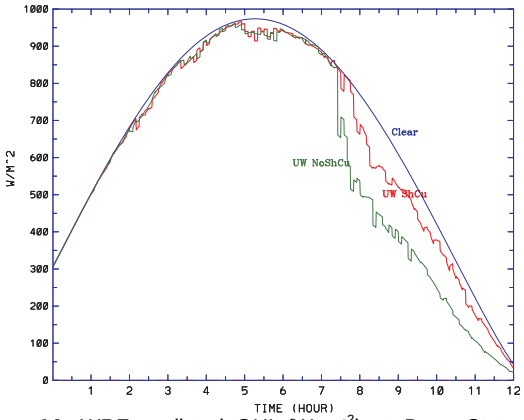

Figure 14. *WRF-predicted GHI (W m^{-2}) at Penn State Rock Springs facility between 12 UTC 30 July 2013 and 00 UTC 31 July 2013. The red curve shows the mode-predicted GHI by WF using the UW SCP scheme and the blue curve shows the WRF-predicted clear-sky values. The green curve shows WRF-predicted GHI values when the UW SCP is turn off (i.e., only with UW PBL, CAM5 MP and KF CPS).*

To evaluate the performance of the UW SCP scheme, same model statistics (MAE and ME) are computed using the same meteorological observations during the simulation period within the entire model domain. The MAE and ME of the ShCu simulation are compared between the baseline evaluation that uses the PSU SCP scheme and the comparison evaluation that uses the UW SCP scheme. Figure 15 shows model error as a function of height for the WRF-predicted temperature, for both 12 and 00 UTC times. It is shown that PSU SCP scheme has a clear advantage in this case in predicting temperature except at the surface for the 24 h time. As mentioned earlier, NBC clouds predicted in the PSU SCP scheme may dissipate too slowly, causing a cold bias at the second morning due to blocking solar radiation.

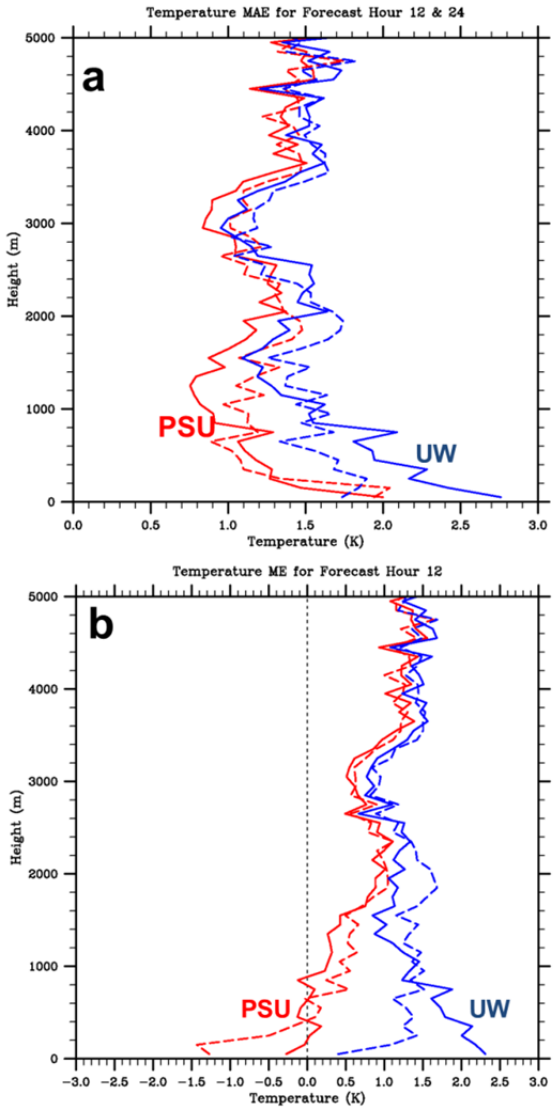

Figure 15. *WRF-predicted temperature, a) MAE and b) ME, as a function of height at 12 h or 00 UTC, 31 July 2013 (solid), and 24 h or 12 UTC 31 July 2013 (dashed). Red curves represent the values from the WRF simulation using the PSU SCP scheme and blue curves from using the UW SCP scheme.*

7. DISCUSSION ON COMPUTING COST

Since the PSU-Deng SCP scheme contains prognostic equations for cloud fraction and cloud water, one would logically wonder how much computing load is added. To address this concern, a timing experiment was conducted. With the same case study, for a model configuration with 48-h simulation on the same 36-km grid, with the same 110x110x50 grid points, the ShCu simulation took 27 minutes and NoShCu simulation took 24 minutes using the same 48 CPU cores. This means that the PSU-Deng SCP scheme adds 12.5% to the computation time. It is worth noting that this computation cost can be reduced by converting many of the thermodynamics calculations to use look-up tables (like other physics schemes in WRF including KF CPS), which could significantly reduce the CPU cost.

8. SUMMARY AND CONCLUSIONS

The PSU-Deng SCP scheme is currently being implemented into the WRF modeling system, along with the PSU GS PBL scheme. After several WRF SCM tests with various convective environments, 3-D evaluation was performed for a continental shallow cumulus case. PSU-Deng SCP is able to produce reasonable cloud fraction, and reduce model temperature bias through radiative interaction with partial cloudiness. Objective evaluation based on ~2000 surface stations and ~60 upper air stations showed that WRF using the PSU SCP scheme shows skill in reducing model errors in both MAE and ME of the model-predicted temperature and moisture. The improved model prediction of temperature is supported by the improved solar radiation flux reaching the ground.

Sensitivity experiment with using MYNN PBL scheme produces similar results, indicating that the PSU SCP scheme is flexible and can be used with a different TKE-based PBL scheme. Compared to using UW SCP, WRF using PSU-Deng SCP produces better verification for both radiation and standard meteorological observations for this case.

Future work includes 1) test at higher horizontal resolution; 2) addition of NBC advection terms which may improve/enhance nighttime cloud dissipation, 3) extension to use with non-TKE based PBL schemes, both TKE and non-TKE based; 4) extensive 3-D evaluations over various convective environments to ensure the robustness; and 5) updates and further improvements (e.g., allowing more sophisticated microphysics, aerosol, tracer mixing, etc.).

9. REFERENCES

Bretherton, C. S, J. R. McCaa, and H. Grenier, 2004: A new parameterization for shallow cumulus convection and its application to marine subtropical cloud-topped boundary layers. Part I: Description and 1D results. *Mon. Wea. Rev.*, **132**, 864-882.

Deng, A., D.R. Stauffer, B.J. Gaudet, J. Dudhia, J. Hacker, C. Bruyere, W. Wu, F. Vandenberghe, Y.

Liu and A. Bourgeois, 2009: Update on WRF-ARW end-to-end multi-scale FDDA system, *10th Annual WRF Users' Workshop*, Boulder, CO, June 23-26, 14 pp (Available on the web at: http://www.mmm.ucar.edu/wrf/users/workshops/WS 2009/abstracts/1-09.pdf).

Deng, A., 1999: A shallow-convection parameterization for mesoscale models, Ph.D Dissertation. The Pennsylvania State University.

Deng, A., N. L. Seaman and J. S. Kain, 2003a: A shallow-convection parameterization for mesoscale models Part I: Sub-model description and preliminary applications. *J. Atmos. Sci.*, **60**, 34-56.

Deng, A., N. L. Seaman and J. S. Kain, 2003b: A shallow-convection parameterization for mesoscale models Part II: Verification and sensitivity studies. *J. Atmos. Sci.*, **60**, 57-78.

Deng A., B. Gaudet, J. Dudhia and K. Alapaty, 2013: Implementing a New Shallow Convection Scheme into WRF, *14th Annual WRF Users' Workshop*, Boulder, CO, June 24-28,9pp (Available on the web at: http://www.mmm.ucar.edu/wrf/users/workshops/WS 2013/extended_abstracts/6.4.pdf).

Grell, G. A., J. Dudhia, and D. R. Stauffer, 1994: A description of the fifth generation Penn State/NCAR Mesoscale Model (MM5). *NCAR Tech. Note NCAR/TN-3981STR*, 138 pp.

Iacono, M., J. Delamere, E. Mlawer, M. Shephard, S. Clough, and W. Collins, 2008: Radiative forcing by long-lived greenhouse gases: Calculations with the AER radiative transfer models, *J. Geo-phys. Res.*, **113**, D13103, doi:10.1029/2008JD009944.

Jakob, C, 2010: Accelerating Progress in Global Atmospheric Model Development through Improved Parameterizations Challenges, Opportunities, and Strategies, *Bull. Amer. Meteor. Soc.*, **91**, 869-875.

Kain, J. S. and J. M. Fritsch, 1990: A one-dimensional entraining/detraining plume model and its application in convective parameterization. *J. Atmos. Sci.,* **47**, 2784-2802.

Kain, J. S. and J. M. Fritsch, 1993: Convective parameterization in mesoscale models: the Kain-Fritsch scheme. *The representation of cumulus convection in numerical models, AMS. Monograph, K.A. Emanuel, and D. J. Raymond, EDS.*, 165-170.

Kain, J. S, 2004: The Kain-Fritsch convective parameterization: An update, *J. Appl. Meteor*, **43**, 170-181.

Shafran, P. C., N. L. Seaman, and G. A. Gayno, 2000: Evaluation of numerical predictions of boundary layer structure during the Lake Michigan Ozone Study (LMOS). *J. Appl. Meteor.*, **39**, 412-426.

Skamarock, W.C., Klemp, J.B., Dudhia, J., Gill, D.O., Barker, D.M., Duda, M.G., Huang, X.-Y., Wang, W., Powers, J.G., 2008. A description of the Advanced Research WRF Version 3. *NCAR Technical Note NCAR/TN-475+STR*. 113 pp.

Xu, K., and D. A. Randall, 1996: A semiempirical cloudiness parameterization for use in climate models. *J. Atmos. Sci.*, **53**, 3048-3102.